THE VERIFICATION METHOD STUDY OF DYNAMIC FLIGHT SIMULATION OF HUMAN CENTRIFUGE

Yifeng LI, Lihui ZHANG, Baohui LI, Cong WANG, Ke JIANG, Minghao YANG, Yi WANG*

Dynamic Flight Simulation (DFS) is an important part of human centrifuge. Because the algorithm and program of DFS system are generally opaque to users, it is complicated and difficult to evaluate its reliability and consistency directly from the system itself. In the paper, first the three methods to evaluate simulation system are made a brief introduction. Then, taking a typical flight action as an example, three methods are applied and compared. The results show that the verification results obtained by grey correlation analysis method and the evaluation method of DFS simulation fidelity based on Radial Basis Function Kernel are basically consistent, especially the newly proposed evaluation method based on Radial Basis Function Kernel achieves more satisfactory evaluation results. Grey correlation coefficient method and evaluation method based on Radial Basis Function Kernel are both firstly applied to the evaluation of DFS, and achieve good results. Human centrifuge can truly reflect the action performance in DFS. The methods have reference significance and application value for the dynamic performances verification and analysis of the other similar equipments.

Keywords: dynamic flight simulation (DFS), verification method, human centrifuge, aircraft model, grey correlation analysis, Radial Basis Function Kernel

1. Introduction

Human centrifuges can realistically simulate flight loads and autonomously provide pilots with a near-real flight sensory experience. As large-scale training devices, they enable pilots to experience the high maneuverability and high-G environment typical of fighter aircraft, and have become the primary ground-based means of generating sustained G-forces in aerospace medicine [1]. The domestic three-axis centrifuge can simulate three-axis overload, serving as a dynamic simulation platform for pilot training [2].The effectiveness of pilot training on a three-degree-of-freedom human centrifuge depends on the centrifuge's control commands. Different phases of tactical flight missions produce varying levels of pilot overload. To better simulate such conditions, control commands must be designed based on the aircraft's flight characteristic

* Air Force Medical Center, PLA, Air Force Medical University, Beijing, China, e-mail: exiuluo_0@163.com

curves during tactical mission execution. Starting from aircraft handling characteristics, this paper establishes a control model for the human centrifuge and then verifies the effectiveness of Dynamic Flight Simulation (DFS).In human centrifuge systems, DFS plays a critical role and best reflects the system's advanced capabilities. DFS on a centrifuge is based on acceleration simulation—a distinctive feature and key advantage [3] that cannot be replicated by other ground-based equipment. DFS itself constitutes a complex simulation system. Since simulation systems often differ significantly from real ones, it is difficult to directly evaluate their reliability from an engineering standpoint. Therefore, various methods are used to assess their dynamic performance. As the direct output of the system, data offer the most intuitive reflection of system characteristics. The continuous parameters recorded by the centrifuge system represent dynamic information in DFS, including three-axis accelerations, velocities, positions, and other flight data during maneuvers such as takeoff, climb, somersault, and hover. These parameters originate both from the aircraft model in dynamic flight and from the centrifuge's own operation. To verify the consistency of the centrifuge's dynamic performance, aircraft model parameters are used as inputs and centrifuge parameters as outputs. By comparing these two parameter sets in the time domain, the dynamic simulation performance of the centrifuge can be validated.

The verification of dynamic performance in simulation systems relies on both subjective evaluation and quantitative methods. This paper first provides a brief introduction to these two approaches. It then focuses on a flight motion sequence encompassing takeoff and climb maneuvers as a case study to examine the consistency of dynamic performance in flight simulation. The verification employs time-domain graphs, grey relational analysis, and a Radial Basis Function (RBF) kernel-based evaluation method. Previous studies have utilized grey relational analysis to assess the credibility of simulation models or to evaluate simulation data [4,5]. Other research has applied time-domain verification to the acceleration performance of flight simulators during level flight [6]. Additionally, grey relational analysis has been used to determine the relative importance and weighting of various factors in simulation systems, such as in modeling satellite navigation under space environment conditions [7]. In practice, simulation and experimental systems often function as black boxes, making them well-suited for grey relational analysis. This method has gained wide recognition and been applied across numerous fields [8], including urban construction [9], healthcare [10], economics [11,12], commerce [13,14], industry [15], agriculture, aviation, and even in multi-stakeholder conflict negotiation and decision-making [16]. In recent years, scholars have refined and optimized the methodology and models of grey relational analysis, enhancing its effectiveness and expanding its applicability [17,18]. However, these studies typically rely on data from designed

simulation systems or flight simulators and often focus on a single specific flight maneuver. In contrast, this study uses data obtained from a real three-axis human centrifuge. Our research applies multiple analytical methods—grey relational analysis and an RBF kernel-based evaluation—to verify and assess the consistency between the human centrifuge's output and actual flight data across multiple flight postures, achieving satisfactory results. This study proposes a Dynamic Flight Simulation (DFS) evaluation framework that integrates subjective evaluation with objective quantitative assessment, combining time-domain graphical analysis, grey relational coefficients, and an RBF kernel-based method. To our knowledge, no similar integrated approach has been previously reported. It represents a novel application of grey relational theory and RBF kernels to evaluate reliability and simulation fidelity in dynamic flight and offers a reference methodology for verifying the dynamic performance of other simulation equipment.

2. Data sources of the study

All data in the study were collected from the domestic AMST-HC-4E human centrifuge with a main arm length of 8.0 meters. When human centrifuge performs DFS, the main arm of centrifuge rotates around the axis, and centrifuge cabin performs a tri-axial rotation according to the tri-axis accelerations instruction parameters. The subject in cabin also follows a tri-axial rotation and is subjected to the action of +Gz acceleration, that is the centrifuge force from head to foot. The schematic diagram of centrifuge rotation, tri-axis accelerations and subject's body position change is shown in the following Fig. 1.

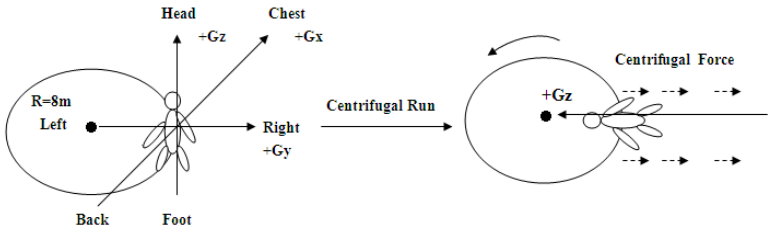

Fig. 1. The schematic diagram of human centrifuge rotation and tri-axial accelerations

The human centrifuge workstation comprises four workstations: medical station, engineering station, DFS station, and recording station. The recording computer at the recording station records and replays numerous parameters of the centrifuge during each centrifuge run, including aircraft model parameters, centrifuge input and output parameters, and various control parameters. When performing the centrifuge dynamic flight simulation, pilot manipulates the control stick, throttle, etc., and outputs electrical signals; and real-time simulation system resolves the aircraft response based on each input signal, generates control target instructions such as target G value, target attitude angle, and angular

velocities and so on, and send them to the motion control system, which is implemented by the multi-axis motion controller to achieve high-speed and precise synchronous motion control, and drives the three-axis motion of the centrifuge. Encoders, gyroscopes and other sensors feed back the actual motion data to the simulation system through the motion controller or PLC, forming a closed loop control. The aircraft model data is generally obtained from the simulation system, and the centrifuge output parameters are obtained from the actual measurement of the sensors. Data is collected synchronously by a high-speed real-time network and a data acquisition system. All data, including manipulation inputs, aircraft conditions, actual motion of centrifuge, and system conditions, etc, are synchronously recorded to a data storage unit for later playback and analysis and so on. During centrifuge running, video data and operational data are packaged and jointly recorded in a designated folder on the cloud drive. The system samples all parameters at a frequency of 200 Hz.. When needed, the aircraft parameters and centrifuge parameters corresponding to a typical flight action of the aircraft are selected, and the parameters are exported in the required format through recording software for subsequent drawing and analysis.

3. The validity verification of typical flight actions

Taking a typical flight action in DFS as an example, the effectiveness of centrifuge simulation is verified through three methods: graphics, grey correlation coefficient, and the evaluation method based on Gaussian kernel model.

3.1 The validity evaluation based on time domain graphics

The performance of Dynamic Flight Simulation (DFS) is primarily reflected in two aspects: the maneuverability of the aircraft during various flight motions, and the dynamic response performance of the centrifuge. In this paper, taking the accelerating takeoff and climbing maneuvers as an example, the dynamic flight performance is verified using a graphical method.

The correlation between the three-axis acceleration curves of the aircraft model and those of the centrifuge is examined. Time domain plots of the three axis accelerations from both the aircraft model and the centrifuge are generated. During DFS, the recording system captures the simulated flight trajectory together with multiple flight parameters. By reviewing the video recorded during the simulation, the occurrence time of each flight motion is carefully identified starting from the initial point marked on the curves. The flight data are then segmented, with each segment containing one or several flight maneuvers, and corresponding parameter curves are plotted. As shown in Fig. 2, at 20 s the aircraft accelerates for takeoff; at 73 s it increases its angle of attack to climb; and at 115 s

it again raises the angle of attack for a subsequent climb. These key moments are annotated in the Fig. 2.

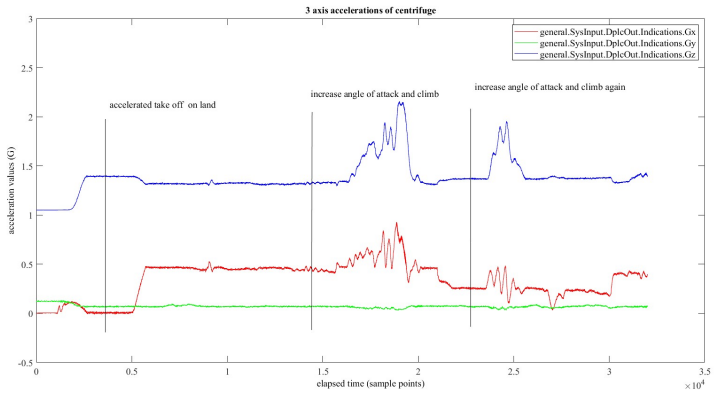

Fig. 2. Three axial accelerations curves graph of centrifuge in accelerating taking off and climbing

In Fig. 2, curves identifications-general. SysInput.DPlcOut. Indications. Gz,general.SysInput.DPlcOut.Indications.Gx, general. SysInput.DPlcOut. Indications.Gy are the three axial accelerations data of centrifuge output.

In Fig. 3, curves identifications-subject001.MSIout.Motion.f_x_b, subject001.MSIout.Motion.f_y_b, subject001.MSIout.Motion.f_z_b are the three axial accelerations data of aircraft model output. Similarly, the corresponding curves graphs of other each parameter can also be made out.

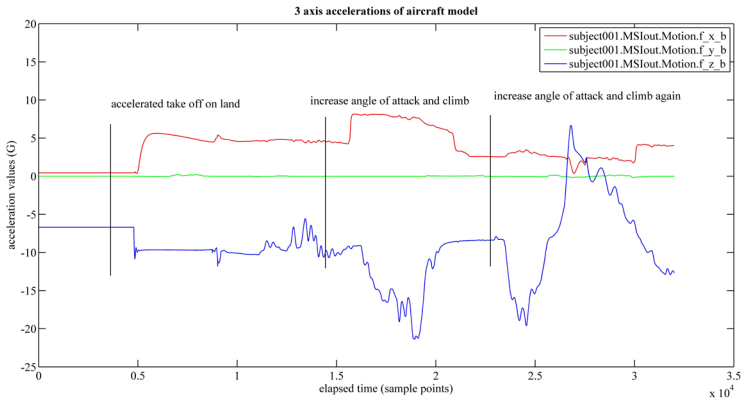

Fig. 3. Three axial accelerations curves graph of aircraft model in accelerating taking off and climbing

From Fig. 3, it can be observed roughly that all three axial accelerations undergo an initialization phase during the aircraft's ground acceleration for takeoff. Correspondingly, the centrifuge operates around a baseline of approximately 1.4 G. During this acceleration, the y-axis acceleration remains relatively small, while the x-axis acceleration is comparatively larger. The trend of the x-axis curve aligns more closely with that of the z-axis curve. These observations indicate that the increase in x-axis acceleration is closely related to

and to some extent driven by the increases in z-axis and y-axis accelerations. Specifically, the growth in z-axis motion contributes to the rise in x-axis motion, while y-axis motion provides a compensatory effect. Although the graphical method reveals the dependencies among the three axes, further quantification of the correlation between the aircraft model and centrifuge motions requires the application of grey relational analysis for a more detailed investigation.

3.2 The validity verification based on grey correlation coefficient

3.2.1 Method introduction

The Fig. 2 and Fig. 3 above provide an intuitive display of the tri-axial acceleration curves. To quantify the relationships between these curves, grey relational analysis is applied to equal-length segments of the data which is presented in the above Fig. 2 and Fig. 3, calculating correlation coefficients to evaluate their interdependencies. The fundamental principle of grey relational analysis is to assess the closeness of relationships between sequences based on the similarity of their geometric shapes. Curves that are more similar in shape correspond to higher correlation degrees, while greater differences indicate lower correlation [19-21]. This method analyzes geometric proximity without considering amplitude differences, which necessitates dimensional consistency in the input data through normalization [4].In practice, grey relational analysis is often used to compare actual data with simulation data. A grey relational coefficient is first computed, followed by an overall grey relational degree, which reflects how well the simulation model matches the actual system. A higher relational degree indicates better agreement [5]. This approach is computationally efficient; however, it does not account for the average spatial distance between data series or their relative positions in space, and requires the original data sequences for evaluation [7].In this study, grey relational analysis is employed to assess the correlation between the model data and centrifuge data in DFS, thereby evaluating the dynamic performance of the simulation.

The steps are as follows:

1) Defining data sequences: Include the output sequence from the actual centrifuge system and the output sequence from the aircraft model generated by the DFS system;
2) Normalize the data: Transform each sequence to a common scale via initialization or dimensionless processing. In this case, the averaged sequence$x_t(i)$ represents the reference data (aircraft model output), while$y_t(i)$ denotes the simulation system output under the ith experimental condition or influencing factor;

3) Compute the grey correlation coefficients: In the grey relational space, calculate the coefficient$\rho_t(i)$ between $x_t(i)$ and $y_t(i)$. The formula is as the following:

$$\rho_t(i) = \frac{\min_i \min_t |y_t(i)-x_t(i)| + \varepsilon * \max_i \max_t |y_t(i)-x_t(i)|}{|y_t(i)-x_t(i)| + \varepsilon * \max_i \max_t |y_t(i)-x_t(i)|} \quad (1)$$

Where $\varepsilon \in (0,1]$ is the resolution coefficient. The smaller the value is, the higher resolution of correlation coefficient is; generally $\varepsilon = 0.5$ is used.

4) Calculate the grey correlation degree: The overall correlation degree $\rho(i)$ is obtained by:

$$\rho(i) = \frac{1}{n}\sum_{i=1}^{n} \sigma_i \rho_t(i) \quad (2)$$

Here σ_i is a weight function chosen according to the specific problem. $\rho(i)$ is the grey correlation degree. Grey relational analysis is well suited for small sample sizes, imposes no strict requirements on sample length or distribution, and is straightforward to implement. It doesn't focus on the relative position of the two series of curves, but more on the similarity degree and changing trend of the two series of curves, that is, the correlation between them, making it particularly appropriate for evaluating correlation degree between time-series curves.

5) Model credibility assessment: If a correlation threshold is defined, $\rho(i)$ with this correlation degree threshold is compared to validate the credibility of the simulation model.

3.2.2 Results and analysis

The correlation coefficient represents the degree of association between two data series at each time point. Using the formula introduced earlier, these time-specific coefficients are aggregated into a single value—the mean correlation degree—which serves as a quantitative measure of the overall relationship between the two series, thereby reflecting the similarity between their corresponding curves. Table 1 presents the correlation degrees between the three axis accelerations of the aircraft model and those of the centrifuge. Here, fx, fy, fz denote the three axis accelerations of the aircraft model, while Gx, Gy, Gz represent the corresponding accelerations of the centrifuge. As the control input to the entire system, the forward-backward and left-right movements of the control stick should also exhibit a strong correlation with the motion output of the centrifuge. Therefore, Table 2 provides the correlation degrees between the

control stick inputs and the three axis centrifuge accelerations. In both tables, the resolution coefficients are set to $\varepsilon = 0.5$.

Table 1

The table of correlation degrees between the three axial accelerations of aircraft model and the three axial accelerations of centrifuge

grey correlation degree	Gx	Gy	Gz
fx	0.7565	0.6721	0.5918
fy	0.8197	0.8196	0.8199
fz	0.6908	0.7551	0.7943

Table 2

The table of correlation degrees between the steering rod and the three axial accelerations of the centrifuge

grey correlation degree	fx	fy	fz	Gx	Gy	Gz
back-forth movement of steering rod	0.8287	0.8115	0.8209	0.8302	0.8078	0.8191
left-right movement of steering rod	0.9215	0.9140	0.9209	0.9213	0.9222	0.9232

The correlation strength is evaluated according to the size of the grey correlation coefficient r, and generally, $r \geq 0.9$ is considered highly correlated, $0.8 \leq r < 0.9$ is strongly correlated, $0.7 \leq r < 0.8$ is moderately correlated, $0.6 \leq r < 0.7$ is weakly correlated and $r < 0.6$ is extremely weakly correlated. As can be seen from the data in Table 1, the lowest correlation value is 0.59, that is fx-the axial acceleration of the aircraft model, and Gz-the axial acceleration of the centrifuge, the correlation between them is the weakest 0.5918 aside, most of the correlation coefficients are above 0.8, which is a strong correlation, especially the data in the second table, which is more obvious. This indicates that the curve shape of the aircraft running curve in accelerating taking off and climbing is more consistent with that of the centrifuge running curve, and there is a strong correlation degree between the three axial accelerations of aircraft model and centrifuge. The correlation degree between the y axis acceleration of aircraft and the three axial accelerations of centrifuge is the strongest. The correlation degrees are all stronger between the accelerations of y axis and z axis of aircraft correlated with the accelerations of the corresponding axis of centrifuge. Combined with the above observation and speculation results by graphic method, x axis motion of aircraft comes more from the z axis motion of centrifuge, and y axis motion is used as compensation. However, the calculation result of correlation degree shows that, x axis acceleration the operator of the steering rob feels more obviously in taking off, fx, comes more from the y axis motion of centrifuge, not the z axis motion. At the same time, it also shows that the quantitative method can achieve the effect that the graphical method can't achieve.

As can be seen from the data in Table 2, the curves shapes of the cockpit stick motion and the three axial accelerations of the aircraft and centrifuge are

more consistent and the correlations between them are strong. Compared with the front-back motion, the correlation degree of the left-right motion of the steering rob and three axial accelerations is stronger, that is, the left-right motion of the steering rob has a more acute output response. The data in the table shows that the correlation between steering rod activity and accelerations of centrifuge is stronger than that of aircraft model, which is not completely consistent with the actual application. Because the steering rod is the input and the centrifuge is the final output, and the steering rod activity should be more closely related to the aircraft. In this case, the result is not quite consistent with the practical application, which may be related to the flight motion. By analyzing of other flight movements, the result shows that there is a stronger correlation degree between steering rob and aircraft model.

3.3 The evaluation of DFS simulation fidelity based on Radial Basis Function Kernel

3.3.1 Theoretical background

To evaluate the similarity between the centrifuge-simulated aircraft attitude and the actual aircraft attitude, a method based on the Gaussian kernel is employed. The Gaussian kernel is a widely used kernel function, primarily applied in machine learning and pattern recognition—particularly in Support Vector Machines (SVMs). It maps data into a high-dimensional feature space, where originally linearly inseparable data may become separable. The fundamental principle of the Gaussian kernel is to measure the "distance" between two data points in this feature space. This distance is computed using a Gaussian function, also known as a radial basis function, defined as follows:

$$K(x, y) = exp\left(-\frac{\|x-y\|^2}{2\sigma^2}\right) \tag{3}$$

In the equation above, **x** and **y** represent two data points in the input space, while α denotes a free parameter that controls the bandwidth (or width) of the Gaussian function. A larger α results in a smoother distribution of the function in the feature space, whereas a smaller α leads to a sharper distribution.

3.3.2 Methods and steps

(1) Data preprocessing: The aircraft model data and centrifuge data are normalized by subtracting the mean and scaling to unit variance to eliminate dimensional effects.

(2) Gaussian kernel computation: For each channel, the Gaussian kernel is computed between corresponding normalized data points.

(3) Similarity scoring: The similarity score is derived by averaging the Gaussian kernel values across the series. Multiple σ values are tested, and the score corresponding to the highest similarity is selected. A higher score indicates closer agreement between simulated and real data.

The similarity score S for two time series X and Y is calculated as follows:

$$S = \frac{1}{n}\sum_{i=1}^{n} K(x_{i,}y_i) \tag{4}$$

Where n is the length of the time series, and x_i and y_i represent the values of X and Y at the i-th time point respectively. By averaging the Gaussian kernel outputs, a similarity score in the range [0,1] is obtained, with higher scores indicating greater similarity between the simulated and real data.

3.3.3 Results and analysis

Taking the aforementioned typical maneuvers as an example, similarity scores between the aircraft model and the centrifuge were calculated for the x, y, and z axes. Here, fx, fy, fz denote the three-axis accelerations of the aircraft model, while Gx, Gy, Gz represent the corresponding accelerations measured on the centrifuge. The x, y, and z axes correspond to three distinct measurement channels.The best RBF similarity scores obtained are 0.9992, 0.9933, and 0.9848, respectively. These values indicate a high degree of similarity between the centrifuge-simulated aircraft attitude and the real aircraft attitude data across all three channels. A score close to 1 reflects strong overall shape agreement between the two time series. Specifically, the x direction simulation, with a score of 0.9992, shows near-perfect consistency with the real data, suggesting that the centrifuge model accurately reproduces the aircraft's dynamic behavior in this axis. This finding aligns with the earlier conclusion drawn from the grey relational coefficient method. Similarities in the other directions, though slightly lower than that of the x axis, still demonstrate a strong correspondence between the simulation and the actual measurements. Overall, the results confirm that the proposed evaluation method achieves better performance in assessing simulation fidelity compared to the conventional grey relational coefficient approach.

Fig. 4 illustrates the variation of RBF similarity scores across the three channels under different σ values. The similarity score for each channel is represented by a distinct colored curve. The horizontal axis denotes the bandwidth parameter σ of the Gaussian kernel function, while the vertical axis represents the normalized similarity score, ranging from 0 to 1. A higher score indicates greater similarity between the corresponding time series. As shown in the Fig. 4, the similarity scores for all channels tend to stabilize as σ increases, suggesting that within a certain range, the influence of σ on the similarity score is relatively limited. Among all σ values, Channel 1 consistently achieves the highest

similarity score, remaining close to 1, which reflects an almost identical shape between its time series and the reference sequence. The similarity scores for Channel 2 and Channel 3, though slightly lower than that of Channel 1, still demonstrate a high degree of similarity, with scores exceeding 0.98.When σ is small (e.g., 0.1 and 0.5), the similarity score exhibits noticeable fluctuation, likely due to the heightened sensitivity of the Gaussian kernel to small-scale differences at narrow bandwidths. These results confirm that the aircraft attitude simulated by the centrifuge closely matches the real aircraft attitude in overall shape, particularly along the x axis (Channel 1). Furthermore, Fig. 4 underscores the importance of selecting an appropriate σ value in Gaussian kernel-based similarity calculations.

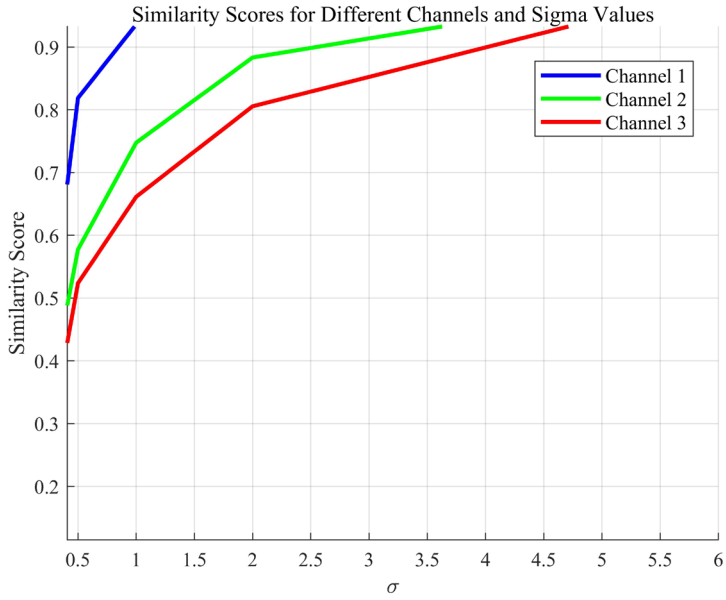

Fig. 4. The curves graph of similarity scores for different channels with sigma change

Fig. 5 displays the RBF similarity scores in the form of a heat map across different Gaussian kernel bandwidths σ. The three aircraft parameters and the three centrifuge parameters are each treated as separate channels, resulting in a total of six channels. As observed, lower σ values generally correspond to higher similarity scores. For σ in the range of [0.1, 0.5], across channels 1–3, the values predominantly fall within the yellow region (score ≈ 0.9). This indicates that a narrow bandwidth is more sensitive to local dynamic variations, thereby imposing a stricter fidelity evaluation. Among these, Channel 1 maintains the highest similarity (≈ 0.9) across the entire σ range, followed by Channel 2. In contrast, channels 4 – 6 are generally shaded in blue (score ≈ 0.2 – 0.4), suggesting lower simulation accuracy and reproducibility in the corresponding degrees of freedom. Beyond σ ≥ 2, the scores stabilize across all channels. The

rapid convergence of scores with increasing σ indicates that once the kernel width exceeds 2, further amplification of dynamic differences is negligible—a phenomenon that can be regarded as the "over-smoothing" threshold.

In summary, the heat map not only provides an intuitive optimal range for selecting σ (0.1–0.5), but also clearly identifies weaker simulation channels, offering a quantitative basis for targeted improvements in future work.

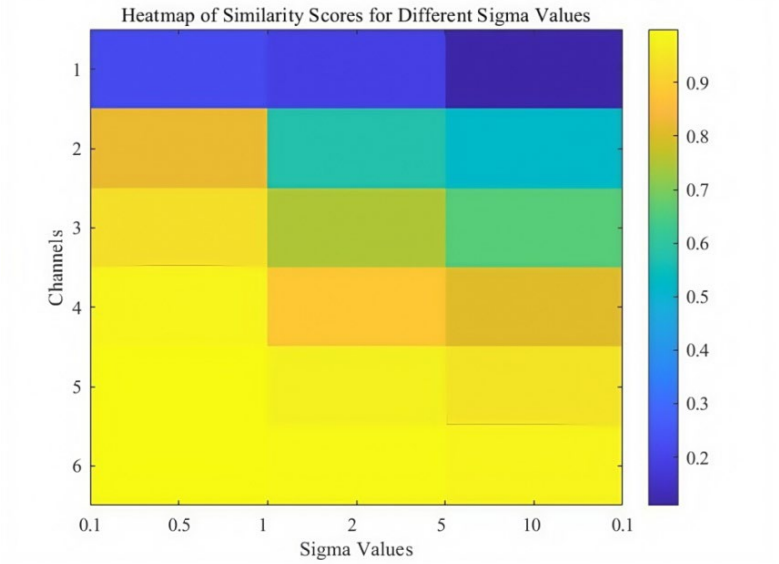

Fig. 5. Heat map of similarity scores for different sigma values

4. Conclusions

Dynamic Flight Simulation (DFS) is a crucial component of human centrifuge systems. As the scale and complexity of simulation systems continue to grow, the verification and evaluation of DFS become increasingly challenging. This paper briefly introduces three methods for verifying the dynamic performance of simulation systems, using a typical flight maneuver as an example to illustrate their application. Among these, the grey relational coefficient method and the DFS fidelity evaluation method based on the Radial Basis Function (RBF) kernel yield particularly satisfactory results. The findings confirm the effectiveness of the proposed control model and demonstrate that the human centrifuge simulation platform can effectively reproduce pilot overload, thereby providing high quality DFS task training. The same methodology can be extended to verify the flight performance of other aircraft maneuvers. This approach is suitable not only for credibility assessment of the overall simulation system, but also for evaluating individual subsystems. It should be noted that the current study analyzes fidelity primarily from the perspective of curve shape and trend consistency. However, the fidelity of DFS should also be examined from the

standpoint of motion perception. An accurate motion perception model—especially an angular motion perception model—is essential for designing kinematic calculation algorithms. Given that motion perception characteristics are difficult to quantify directly, future experimental studies could focus on temporal and phase characteristics to conduct parameter identification for such perception models. This paper suggests that by establishing an angular motion perception model, identifying and optimizing individual perceptual parameters, and subsequently enhancing DFS fidelity, it is possible to customize and refine kinematic calculation algorithms for human centrifuges. This would lay the groundwork for further personalized algorithm design in DFS applications. These steps represent important follow-up work and will likely form a key research focus—and challenge—in advancing DFS technology. Finally, the verification and evaluation methodology presented here can be extended to performance assessment in other dynamic flight simulations, and offers reference value for the fidelity evaluation of DFS in other simulation based training systems.

REFERENCES

[1]. *Navid Mohajer, Asher Winter, Timothy Mark Gregory, et al*, "Experimental Validation of a High-G Centrifuge System using an Advanced Wireless Human Dummy". Proceedings of 2022 IEEE International Conference on Systems, Man, and Cybernetics, 2022:2827-2833.

[2]. *Yifeng Li, Ke Jiang, Baohui Li, et al*, "Basic structure, principles and troubleshooting of high-performancehuman centrifuge". Chinese Medical Equipment Journal, vol. 42, no. 07, 2021, pp. 97-99+103.

[3]. *Scott J. Wood, R. Tyson Lathan, & K. Erik Britton*, Human centrifuge training for space flight. Journal of Vestibular Research, 19(5-6), 2009, 225-235, DOI: https://doi.org/10.3233/VES-2009-0361.

[4]. *Boyuan Liu, Jiahui Jiang, Wenhui Fan, Huiyang Qu, Baocun Hou*, "Credibility Evaluation of Simulation Data Based on Grey Correlation Analysis", System Simulation Technology, vol. 10, no. 1, 2014, pp. 32-35.

[5]. *Zhao Lu, Xiaoguang Fan,Guodong Li, Chongwang Yue*, "A Modeling C r edibility Validation Algoithm Based On G r ey R elational Analysis". Computer Applications and Software, vol. 30, no. 12, 2013, pp.252-254. DOI: 10. 3969 /j. issn. 1000-386x. 2013. 12. 066.

[6]. *Zhe Wang,Guo-hui Li,Shan-lu Zhao*, "Dynamic Performance Time Domain Verification Analysis of a Flight Simulator", Modern Computer, no.11,2017, pp.34-37. DOI:10.3969/j.issn.1007-1423.2017.32.008.

[7]. *Lifeng Zheng, Jianbing Tang*, "Weight Determination of Assessment Indices in System Simulation Based on Gray Correlation Analysis", Computer Simulation, vol. 24, no. 9, 2007, pp.76-78.DOI:10.3969/j.issn.1006-9348.2007.09.022.

[8]. *Arican, Özlem İlksen, Cengiz Kahraman,* "Grey Relational Analysis, Ranking and Applications: A Literature Review.",Grey Systems: Theory and Application, vol. 13, no. 4, 2023, pp. 761-98,DOI: https://doi.org/10.1108/GS-03-2023-0021.

[9]. *Deveci, Muhammet, Gokasar, Ilgin, Pamucar, Dragan, & Köppen, Mario, "*A fuzzy grey relational analysis approach for the evaluation of urban mobility projects in the context of smart cities", Engineering Applications of Artificial Intelligence, 123(Part A), 2023, 106228, DOI: https://doi.org/10.1016/j.engappai.2023.106228.

[10]. *Kumar, Anil, & Sharma, Rohit,* Evaluating healthcare service quality during pandemics using grey relational analysis: A comparative study of public and private hospitals, Operations Management Research, 16(2), 2023, pp.1023-1041, DOI: https://doi.org/10.1007/s12063-023-00379-8.

[11]. *Ouali, Makhlouf, Ramzan, Bashir, Hanif, Muhammad Waqas, Bhatti, Ghulam Abbas, Nawaz, Muhammad*, "Growth of Digital Infrastructure of China and USA: Application of Intelligent Grey Forecasting Model. International Journal of Grey Systems", vol. 4, no. 2, 2024, pp. 23-31. DOI: https://doi.org/10.52812/ijgs.101.

[12]. *Makhlouf Ouali, "*Studying Foreign Trade and Economic Growth of Morocco using Regression and Grey Relational Analyses", International Journal of Grey Systems, vol. 3, no. 2, 2023, pp.8-29. DOI: https://doi.org/10.52812/msbd.79.

[13]. *Torkayesh, Ali Ebadi, & Deveci, Muhammet,* A hybrid grey relational analysis and double normalization-based multi-aggregation (DNMA) model for sustainable circular supplier selection,*Annals of Operations Research, 332*(1), 2024,pp. 515-549,DOI: https://doi.org/10.1007/s10479-022-05007-5.

[14]. *Petro Bulanyi (Family Name),Alinafe Kaliwo(Family Name)*,"Evaluation of Barriers to E-commerce in Malawi using Grey Relational Analysis", International Journal of Grey Systems, vol. 3, no. 1, 2023, pp.5-16,DOI: https://doi.org/10.52812/ijgs.67.

[15]. *Luefeng. Chen, Kuanlin. Wang, Min. Li, Min. Wu, Witold. Pedrycz and Kaoru. Hirota*, "K-Means Clustering-Based Kernel Canonical Correlation Analysis for Multimodal Emotion Recognition in Human-Robot Interaction," in IEEE Transactions on Industrial Electronics, vol. 70, no. 1 , pp. 1016-1024, Jan. 2023, doi: 10.1109/TIE.2022.3150097.

[16]. *Yong. Liu, Qin. Jiang, Zi Hong. Huang and Jeffrey Yi-Lin Forrest*, "A Multiobjective Super Conflict Grey Target Negotiation Consensus Approach," in IEEE Transactions on Systems, Man, and Cybernetics: Systems, vol. 54, no. 7, pp.3934-3948, July 2024, doi: 10.1109/TSMC.2024.3374340.

[17]. *Sifeng Liu, Wenqing Wu, Yingjie Yang, Zhigeng Fang, "*Posterior variance test: ex ante evaluation of grey forecasting model", International Journal of Grey Systems, vol. 3, no. 1, 2023,pp.17 - 28, DOI: https://doi.org/10.52812/ijgs.71 2 .

[18]. *Nowak Marcin, Pawłowska-Nowak, Marta, Koko cińska, Małgorzata, & Kułyk Piotr*, "The evaluation of grey relative incidence", Grey Systems: Theory and Application, 2023, vol. 14, no. 2, pp.263 - 282. DOI: https://doi.org/10.1108/gs - 06 - 2023 - 0049.

[19]. *Michael Gr. Voskoglou*, "Grey assessment", International Journal of Grey Systems, vol. 3, no. 2, 2023, pp.5-7, DOI: https://doi.org/10.52812/ijgs.77.

[20]. *Preston Briggs, Keith D. Cooper, Linda Torczon*, "Improvements to graph coloring register allocation", ACM Transactions on Programming Languages and Systems, vol. 16, no. 3, 1994, pp.428－455． DOI: 10.1145/177492.177778.

[21]. *Xiwei Guo and Christiantine Della*, " The construction of an index system for measuring photography teaching literacy in universities based on grey correlation analysis in cross-cultural teaching ",Applied Mathematics and Nonlinear Sciences, vol. 9, no. 1,2024, pp.1-18,DOI: https://doi.org/10.24746/amns.2024.1003.